

A Decade of Radial-Velocity Discoveries in the Exoplanet Domain

Stéphane Udry
Geneva University

Debra Fischer
San Francisco State University

Didier Queloz
Geneva University

Since the detection of a planetary companion orbiting 51 Peg one decade ago, close to 200 extrasolar planets have been unveiled by radial-velocity measurements. They exhibit a wide variety of characteristics, including large masses with small orbital separations, high eccentricities, multiplanet architectures, and orbital period resonances. Here, we discuss the statistical distributions of orbital parameters and host star properties in the context of constraints they provide for planet-formation models. We expect that radial-velocity surveys will continue to provide important discoveries. Thanks to ongoing instrumental developments and improved observing strategies, Neptune-mass planets in short-period orbits have recently been detected. We foresee continued improvement in radial-velocity precision that will reveal Neptune-mass planets in longer-period orbits and planets down to a few Earth masses in short-period orbits. The next decade of Doppler observations should expand the mass distribution function of exoplanets to lower masses. Finally, the role of radial-velocity followup measurements of transit candidates is emphasized.

1. INTRODUCTION

Before 1995, the solar system was the only known example of a planetary system in orbit around a Sun-like star, and the question of its uniqueness was more a philosophical than a scientific matter. The discovery of an exoplanet orbiting the Sun-like star, 51 Peg (*Mayor and Queloz, 1995*), changed this fact and led to a steadily increasing number of exoplanet detections. During the ensuing years, we learned first that gas giant planets are common and that the planetary-formation process may produce a surprising variety of configurations: masses considerably larger than Jupiter, planets moving on highly eccentric orbits, planets orbiting closer than 10 stellar radii, planets in resonant multiplanet systems, and planets orbiting components of stellar binaries. Understanding the physical reasons for such wide variations in outcome remains a central issue in planet-formation theory. The role of observations is to provide constraints that will help theoreticians to model the large variety of properties observed for extrasolar planets.

From the mere 7 or 8 exoplanets known at the time of the Protostars and Planets IV conference [and the 17 candidates published in the proceedings (*Marcy et al., 2000*)], the number of known exoplanets has now surpassed 200. With this larger sample, statistically significant trends now appear in the distribution of orbital elements and host-star properties. The features of these distributions are fossil traces of the

processes of formation or evolution of exoplanet systems and help to constrain the planet-formation models.

Here we present a census of the main statistical results obtained from spectroscopic observations over the past decade. In addition to the orbital properties described in sections 2 and 4, and the primary-star characteristics discussed in section 5, we will discuss the evolution of radial velocity measurements over the past two years, namely (1) the role played by followup radial-velocity measurements in confirming and characterizing planetary objects among the many candidates detected by photometric-transit programs (section 6) and (2) the development of specially designed high-resolution spectrographs achieving precisions for radial velocities below the 1 m s^{-1} limit (section 3). This extreme precision opens the possibility for detection of Earth-type planets with radial-velocity measurements (section 7).

2. ORBITAL PROPERTIES OF EXOPLANETS

As a result of the increase in the temporal baseline of the large radial-velocity planet searches (Lick, Keck, AAT, ELODIE, CORALIE programs) and the initiation of new large surveys [e.g., HARPS planet search (*Mayor et al., 2003*)] and metallicity-biased searches for hot Jupiters (*Fischer et al., 2005; Da Silva et al., 2006*), there is a large sample of known extrasolar planets. This lends some confidence to observed trends in statistical distributions of the

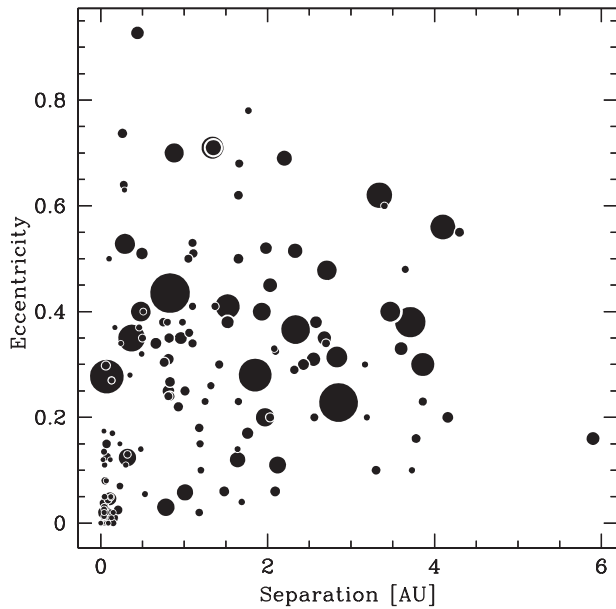


Fig. 1. Separation-eccentricity diagram for the complete sample of presently known extrasolar planets. The size of the dots is proportional to the minimum mass of the planet candidates ($m_2 \sin i \leq 18 M_{\text{Jup}}$).

planet properties. The most remarkable overarching feature of the sample is the variety of orbital characteristics. This variety challenges the conventional views of planetary formation. A global visual illustration of these properties is given in Fig. 1, displaying orbital eccentricities as a function of planet-star separations for the complete sample of known extrasolar planets. Several of the planet properties (close proximity to the star, large eccentricity, high mass) are clearly apparent in the figure. The goal now is to interpret the observed orbital distributions in terms of constraints for the planet-formation models.

The determination of statistical properties of giant planets should be derived from surveys that are themselves statistically well defined (e.g., volume limited) and that have well-understood detection thresholds in the various planet, primary-star, and orbital parameters. There are several programs that meet these requirements, including the volume-limited CORALIE planet-search program (*Udry et al., 2000*) and the magnitude-limited FGKM Keck survey (*Marcy et al., 2005*). In the diagrams, we present detected planet candidates from all radial-velocity surveys and note that the discussed properties agree with those presented from single well-defined programs as well.

2.1. Giant Extrasolar Planets in Numbers

The most fundamental property that can be obtained from a planet-search program is the fraction of surveyed stars that host detected planets. Given a typical Doppler precision of a few meters per second and duration of observations, this planet occurrence rate is only defined for a

particular parameter space: planets with masses larger than m_{lim} and orbital periods shorter than P_{lim} . The minimum rate is obtained just by counting the fraction of stars hosting planets in this particular slice of parameter space. For planets more massive than $0.5 M_{\text{Jup}}$, *Marcy et al. (2005)* find in the Lick+Keck+AAT sample that $16/1330 = 1.2\%$ of the stars host hot Jupiters ($P \leq 10$ d, i.e., $a \leq 0.1$ AU for a solar-mass star) and 6.6% of stars have planets within 5 AU. In the volume-limited CORALIE sample (including stellar binaries), for the same m_{lim} , we count $9/1650 = 0.5\%$ occurrence of hot Jupiters and, overall, that $63/1650 = 3.8\%$ of stars have planets within 4 AU. As binaries with separations closer than $2''$ to $6''$ are usually eliminated from planet-search programs (along with rapidly rotating stars), if we restrict ourselves to stars *suitable* for planet search (i.e., not binary and with $v \sin i \leq 6 \text{ km s}^{-1}$), then we find for CORALIE that $9/1120 = 0.8\%$ of stars have giant planets with separations less than 0.1 AU and $63/1120 = 5.6\%$ of stars have planets at separations out to 4 AU. Within Poisson error bars, and including a correction to account for the smaller separation range considered with CORALIE, these two large samples are in good agreement.

The true occurrence rate of gas giant planets can be better approximated by estimating the detection efficiency (as a function of planet mass and orbital period) using Monte Carlo simulations. This has not yet been done for the largest surveys. However, for the ELODIE program (magnitude-limited sample of stars cleaned from known binaries), although dominated by small number statistics errors, *Naef et al. (2005)* estimate for planets more massive than $0.5 M_{\text{Jup}}$ a corrected fraction $0.7 \pm 0.5\%$ of hot Jupiters with $P \leq 5$ d and $7.3 \pm 1.5\%$ of planets with periods smaller than 3900 d. A similar analysis has been carried out by *Cumming et al. (1999)* for the Lick survey and by *Endl et al. (2002)* for the planet-search program with the ESO Coudé-échelle spectrometer. In the overlapping parameter space, all these analyses show good agreement.

With the continuously increasing time span of the surveys and the improvement in our ability to detect smaller-mass planets, we expect the fraction of stars hosting planets to increase substantially from these estimated minimum values, perhaps to values higher than 50%, taking into account that the number of detected planets is a rising function of decreasing planet masses and the rise in planet detections at wide separations (see sections 2.2 and 2.3).

2.2. Planetary Mass Distribution

Even after the detection of just a few extrasolar planets it became clear that these objects could not be considered as the low-mass tail of stellar companions in binary systems (with low $m_2 \sin i$ because of nearly face-on orbital inclinations). The strong bimodal aspect of the secondary mass distribution to solar-type primaries (Fig. 2) has generally been considered as the most obvious evidence of different formation mechanisms for stellar binaries and planetary systems. The interval between the two populations (the

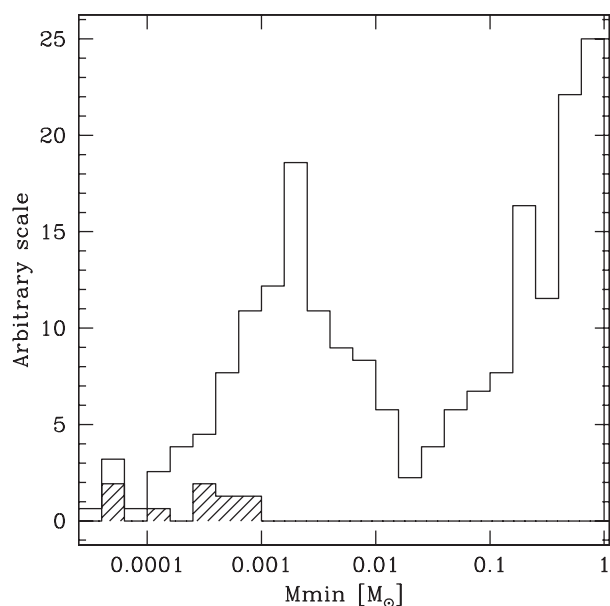


Fig. 2. Minimum mass distribution of secondaries to solar-type primaries. The stellar binaries are from Halbwachs et al. (2003). The hatched histogram represents HARPS planets (section 3).

brown-dwarf desert) corresponding to masses between ~ 20 and $\sim 60 M_{\text{Jup}}$ is almost empty, at least for orbital periods shorter than a decade. However, there is probably an overlap of these two distributions; at this point, it is not easy to differentiate *low-mass brown dwarfs* from *massive planets* just from their $m_2 \sin i$ measurements, without additional information on the formation and evolution of these systems. (A dedicated working group of the IAU has proposed a *working definition* of a “planet” based on the limit in mass at $13 M_{\text{Jup}}$ for the ignition of deuterium burning.)

Toward the low-mass side of the planetary mass distribution, a clear power-law type rise is observed (Fig. 2). Marcy et al. (2005) proposed $dN/dM \propto M^{-1.05}$ for their FGKM sample. This fit is not affected by the unknown $\sin i$ distribution (Jorissen et al., 2001), which simply scales in the vertical direction. The low-mass edge of this distribution is poorly defined because of observational incompleteness; the lowest-mass planets are difficult to detect because the radial-velocity variations are smaller. It is then likely that there is a large population of sub-Saturn-mass planets. This trend is further supported by accretion-based planet-formation models. In particular, large numbers of “solid” planets are expected (Ida and Lin, 2004a, 2005; Alibert et al., 2004, 2005) (see also section 3).

2.3. Period Distribution of Giant Extrasolar Planets

Figure 3 displays the orbital period distribution for the known exoplanet sample. The numerous giant planets orbiting very close to their parent stars ($P < 10$ d) were completely unexpected before the first exoplanet discoveries. The standard model (e.g., Pollack et al., 1996) suggests that

giant planets form first from ice grains in the outer region of the system where the temperature of the stellar nebula is cool enough. Such grain growth provides the supposed requisite solid core around which gas could rapidly accrete (Safronov, 1969) over the lifetime of the protoplanetary disk ($\sim 10^7$ yr). The detection of planets well inside the ice line requires that the planets undergo a subsequent migration process moving them close to the central star (see, e.g., Lin et al., 1996; Ward, 1997; see also the chapter by Papaloizou et al. for an updated review). Alternative points of view invoke *in situ* formation (Bodenheimer et al., 2000; Wuchterl et al., 2000), possibly triggered through disk instabilities (see the chapter by Durisen et al.). Note, however, that even in such cases, subsequent disk-planet interactions leading to migration is expected to take place as soon as the planet has formed. The observed pileup of planets with periods around 3 d is believed to be the result of migration and requires a stopping mechanism to prevent the planets from falling onto the stars (see, e.g., Udry et al., 2003, and references therein for a more detailed discussion).

Another interesting feature of the period distribution is the rise of the number of planets with increasing distance from the parent star. This is not an observational bias as equivalent mass candidates are more easily detected at shorter periods with the radial-velocity technique. The decrease of the distribution beyond 10 yr coincides with, and is almost certainly a result of, the limited duration of most of the radial-velocity surveys. The overall distribution can

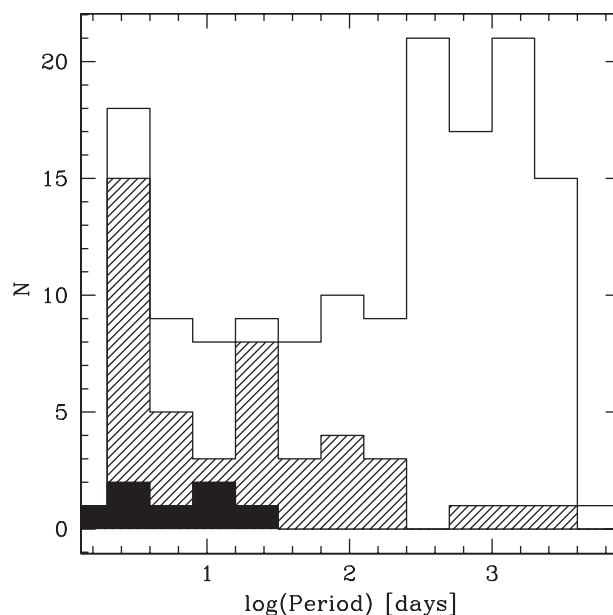


Fig. 3. Period distribution of known gaseous giant planets detected by radial-velocity measurements and orbiting dwarf primary stars. The hatched part of the histogram represents “light” planets with $m_2 \sin i \leq 0.75 M_{\text{Jup}}$. For comparison, the period distribution of known Neptune-mass planets (section 3) is given by the filled histogram. (Note, however, that there is still very high observational incompleteness for these low-mass planets.)

then be understood as being comprised of two parts: a main distribution rising with increasing periods [as for binary stars (*Halbwachs et al.*, 2003)], the maximum of which is still undetermined; and a second distribution of planets that have migrated inward. The visible lack of planets with orbital periods between 10 and 100 d is real, and appears to be the intersection between the other two distributions.

A minimum flat extrapolation of the distribution to larger distances would approximately double the occurrence rate of planets (*Marcy et al.*, 2005). This conservative extrapolation hints that a large population of yet-undetected Jupiter-mass planets may exist between 5 and 20 AU. This is of prime importance for the direct-imaging projects under development on large telescopes such as the VLT or Gemini Planet Finder (see the chapter by Beuzit et al.) and space-based imaging missions such as NASA's Terrestrial Planet Finder or ESA's Darwin.

2.4. Period Mass Distribution

The orbital-period distribution highlights the role of migration processes underlying the observed configuration of exoplanet systems. An additional correlation is seen between orbital period and planet mass. This correlation is illustrated in Fig. 4, showing the mass-period diagram for the known exoplanets orbiting dwarf primaries.

The most obvious characteristic in Fig. 4 is the paucity of massive planets on short-period orbits (*Zucker and Mazeh*,

2002; *Udry et al.*, 2002; *Pätzold and Rauer*, 2002). This is not an observational bias as these candidates are the easiest ones to detect. Even more striking, when we neglect the multiple-star systems (section 2.5), a complete void of candidates remains in the diagram for masses larger than $\sim 2 M_{\text{Jup}}$ and periods smaller than ~ 100 d. The only candidate left is HD 168443 b, a member of a possible multi-brown-dwarf system (*Marcy et al.*, 2001; *Udry et al.*, 2002).

Migration scenarios may naturally result in a paucity of close-in massive planets. For example, type II migration (where the planet clears a gap in the disk) has been shown to be less effective for massive planets; i.e., massive planets are stranded at wider separations than low-mass planets. Alternatively, when a migrating planet reaches small separations from the star, some process related to planet-star interactions could promote mass transfer from the planet to the star, decreasing the mass of the migrating planet (e.g., *Trilling et al.*, 1998), or could cause massive planets to fall into the central star (*Pätzold and Rauer*, 2002).

Another interesting feature of the period distribution is the rise in the maximum planet mass with increasing distance from the host star (Fig. 5) (*Udry et al.*, 2003). While it is true that Doppler detectability for lower-mass planets declines with increasing distance from the star, the massive planets are easily detected at small separations, yet they preferentially reside in more distant orbits. This can be understood in the context of the migration scenario as well. More massive planets are expected to form further out in

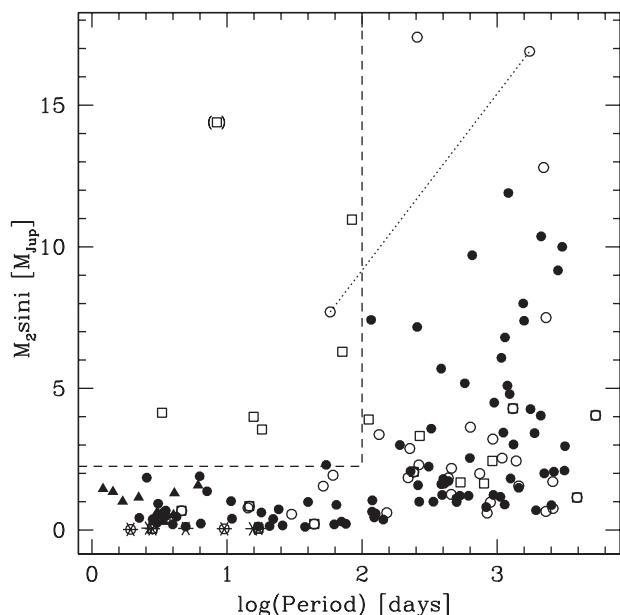


Fig. 4. Period-mass distribution of known extrasolar planets orbiting dwarf stars. Open squares represent planets orbiting one component of a binary system whereas dots are for “single” stars. Open dots represent planets in multiplanet systems. Asterisks represent Neptune-mass planets. Dashed lines are limits at $2.25 M_{\text{Jup}}$ and 100 days. The dotted line connects the two “massive” components orbiting HD 168443.

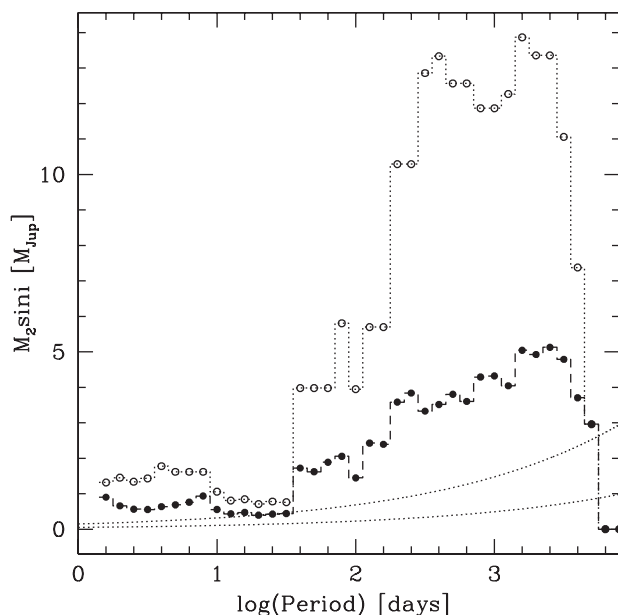


Fig. 5. Mean (filled circle) or highest (average on the three highest values; open circles) mass of planets in period smoothing windows of width $\log P$ (days) = 0.2. Although massive planets are easy to detect in shorter-period orbits, an increase in the maximum planet mass with increasing distance from the star is observed. Detection limits for velocity semi-amplitudes K of 10 and 30 m s^{-1} ($M_1 = 1 M_{\odot}$, $e = 0$) are represented by the dotted lines.

the protoplanetary disk, where raw materials for accretion are abundant and the longer orbital path provides a larger feeding zone. Then, migration may be more difficult to initiate as a larger portion of the disk has to be disturbed to overcome the inertia of the planet. This notion is further supported by the observation that hot Jupiters have statistically lower masses ($m_2 \sin i \leq 0.75 M_{\text{Jup}}$) that may migrate more easily (Fig. 3).

It has also been suggested that multiplanet chaotic interactions preferentially move low-mass (low-inertia) planets either inward or outward in the system, whereas massive (high-inertia) planets are harder to dislodge from their formation site (Rasio and Ford, 1996; Weidenschilling and Marzari, 1996; Marzari and Weidenschilling, 2002; see also the chapter by Levison et al.). One weakness of this hypothesis is that the frequency of short-period planets is difficult to reproduce with reasonable assumptions for these models (Ford et al., 2001, 2003).

As discussed above, the observations empirically point to a decrease in the efficiency of migration with increasing planet mass. Simulations of migrating planets in viscous disks are consistent with this observation (Trilling et al., 1998, 2002; Nelson et al., 2000). Therefore, it seems reasonable to expect that a large number of massive planets may reside on long-period orbits, and yet may still be undetected because of the time duration of the present surveys. Younger primary stars among them, less amenable to radial-velocity searches because of the intrinsic astrophysical noise of the star, will be suitable targets for direct imaging searches (see the chapter by Beuzit et al.). Lower-mass planets could exist on long-period orbits as well; however, these planets are difficult to detect with precisions $\geq 3 \text{ m s}^{-1}$. Low-mass, distant planets orbiting chromospherically quiet stars may be detected with extreme precision radial velocities with demonstrated stability over a decade or more (see section 3).

2.5. Giant Planets in Multiple Stellar Systems

Among the ~ 200 extrasolar planets discovered to date, at least 30 are known to orbit one of the members of a double- or multiple-star system (Patience et al., 2002; Eggenberger et al., 2004; Mugrauer et al., 2004, 2005). These systems cover a large range of binary projected separations: from ~ 20 AU for two spectroscopic binaries to more than 1000 AU for wide visual systems. Although the sample is not large, some differences between planets orbiting binary components and those orbiting single stars can be seen in the mass-period (Fig. 4) and eccentricity-period (Fig. 6) diagrams. As pointed out by Zucker and Mazeh (2002), the most massive short-period planets are all found in binary- or multiple-star systems. The planets orbiting a component star of a multiple-star system also tend to have a very low eccentricity when their orbital period is shorter than about 40 d (Eggenberger et al., 2004). The only exception is the “massive” companion of HD 162020, which is probably a low-mass brown dwarf (Udry et al., 2002). These observations suggest that some kind of migration process has been

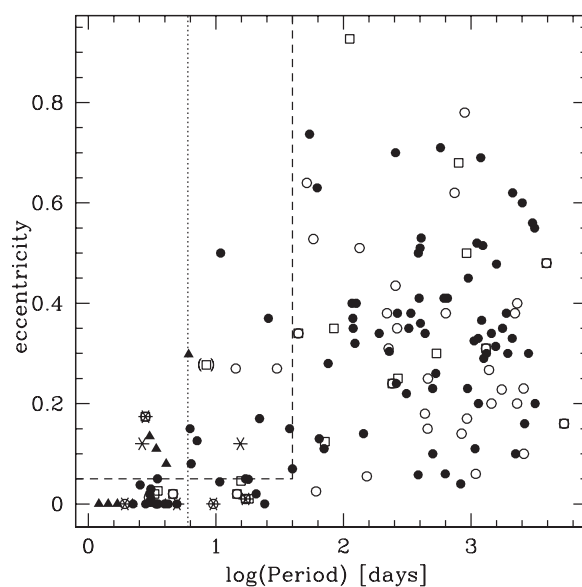


Fig. 6. Period-eccentricity diagram of the known extrasolar planets. Open squares represent planets orbiting one of the components of a binary system whereas dots are for “single” stars. Open dots represent planets in multiplanet systems. Planets detected in metallicity-biased or photometric-transit surveys are indicated by filled triangles. Starred symbols are for Neptune-mass planets. The parentheses “()” locate HD 162020. The dotted line is indicative of an observed tidal circularization period around 6 d (Halbwachs et al., 2005) and the dashed lines limit the $e > 0.05$ and $P < 40$ d domain (see section 2.5).

at work in the history of these systems. The properties of the five short-period planets orbiting in multiple-star systems seem, however, difficult to reconcile with the current models of planet formation and evolution, at least if we want to invoke a single mechanism to account for all the characteristics of these planets.

Even if the stellar orbital parameters for planet-bearing binary stars are not exactly known, we have some information like the projected separations of the systems or stellar properties. No obvious correlation between the properties of these planets and the known orbital characteristics of the binaries or of the star masses are found yet, however. Due to the limitations of the available observational techniques, most detected objects are giant (Jupiter-like) planets; the existence of smaller-mass planets in multiple-star systems is still an open question.

Searches for extrasolar planets using the radial-velocity technique have shown that giant planets exist in certain types of multiple-star systems. The number of such planets is still low, perhaps in part because close binaries are difficult targets for radial-velocity surveys and are excluded from Doppler samples. However, even if the detection and characterization of planets in binaries are more difficult to carry out than the study of planets around single stars, it is still worth doing because of the new constraints and information it may provide on planet formation and evolution. In

particular, circumbinary planets offer a complete unexplored new field of investigations.

2.6. Giant Planet Eccentricities

Extrasolar planets with orbital periods longer than about 6 d have eccentricities significantly larger than those of giant planets in the solar system (Fig. 6). Their median eccentricity is $e = 0.29$. The eccentricity distribution for these exoplanets resembles that for binary stars, spanning almost the full range between 0 and 1. Planets with periods smaller than 6 d are probably tidally circularized (see below).

The origin of the eccentricity of extrasolar giant planets has been suggested to arise from several different mechanisms: the gravitational interaction between multiple giant planets (*Rasio and Ford, 1996; Weidenschilling and Marzari, 1996; Lin and Ida, 1997*); interactions between the giant planets and planetesimals in the early stages of the system formation (*Levison et al., 1998*); or the secular influence of an additional, passing-by (*Zakamska and Tremaine, 2004*), or bounded companion in the system (see *Tremaine and Zakamska, 2004*, for a comprehensive review of the question).

The latter effect seems particularly interesting in some cases. The mean velocity of several planets with eccentric orbits shows a drift, consistent with the presence of a long-period companion. The gravitational perturbation arising from the more distant companion could be responsible for the observed high orbital eccentricity. This effect has been suggested as an eccentricity pumping mechanism for the planet orbiting 16 Cyg B (*Mazeh et al., 1997*). However, *Takeda and Rasio (2005)* have shown that such a process would produce an excessive number of both very high ($e \geq 0.6$) and very low ($e \leq 0.1$) eccentricities, requiring at least one additional mechanism to reproduce the observed eccentricity distribution. In fact, none of the proposed eccentricity-inducing mechanisms alone is able to reproduce the observed eccentricity distribution.

For small periastron distance, giant planets are likely to undergo tidal circularization. For periods smaller than ~ 6 d, nearly all gaseous giant planets are in quasicircular orbits ($e \leq 0.05$; Fig. 6) (*Halbwachs et al., 2005*). The few border cases, with eccentricities around 0.1, have been recently detected with few observations in surveys biased for short-period orbits (metallicity-biased or photometric-transit searches) and have very uncertain eccentricity estimates (even compatible with zero). With more radial-velocity data spanning several orbits, the measured orbital eccentricities may decline. Alternatively, an additional companion may ultimately be found in some of these systems. In multiple-planet systems, a single Keplerian model can absorb some of the longer-period trend in mean velocities, artificially inflating the orbital eccentricity. Additional companions could also tidally pump up eccentricity in short-period systems.

Correlations can also be seen between eccentricity and period, and between eccentricity and mass. The more massive planets (i.e., more massive than $5 M_{\text{Jup}}$) exhibit system-

atically higher eccentricities than do the lower-mass planets (*Marcy et al., 2005*). This cannot be a selection effect (larger induced radial-velocity variation). If planets form initially in circular orbits, the high eccentricities of the most massive planets are puzzling. Such massive planets have the largest inertial resistance to perturbations that are necessary to drive them out of their initial circular orbits. Note that the more massive planets are also found at wider separations (section 2.3), and therefore eccentricity and orbital period are coupled. The long-period planets have usually only been observed for one period and are rarely well covered in phase. This could lead to an overestimate of the derived eccentricity in some Keplerian fits (*Butler et al., 2000*), but overall it seems unlikely that improper modeling is entirely responsible for the observed correlation.

Finally, as seen in Fig. 6, a few long-period, low-eccentricity candidates are emerging from the surveys. They form a small subsample of so-called solar system *analogs*.

3. THE QUEST FOR VERY HIGH PRECISION

3.1. Down Below the Mass of Neptune

After a decade of discoveries in the field of extrasolar giant planets, mainly coming from large high-precision radial-velocity surveys of solar-type stars, the quest for other worlds has now passed a new threshold. Most of the detected planets are gaseous giants similar to our own Jupiter, with typical masses of a few hundreds of Earth masses. However, in the past year, seven planets with masses in the Uranus to Neptune range ($6\text{--}21 M_{\oplus}$) have been detected (Table 1). Because of their small mass and location in the system, close to their parent stars, they may well be composed mainly of a large rocky/icy core, and it is possible that they either lost most of their gaseous atmosphere or simply formed without accumulating a substantial one.

TABLE 1. Summary table for the recently discovered Neptune-mass planets.

Planet	Reference	P (d)	$m_2 \sin i$ (M_{\oplus})	(o-c) (m s^{-1})	q (10^{-5})
μ Ara c	[1]	9.6	14	0.9	4.2
55Cnc e	[2]	2.81	14	5.4	4.7
HD 4308 b	[3]	15.6	14	1.3	5.4
HD 190360 c	[4]	17.1	18	3.5	6.0
Gl 876 d	[5]	1.94	6	4.6	6.0
Gl 436 b	[6]	2.6	21	5.3	16.0
Gl 581 b	[7]	4.96	17	2.5	17.1

The parameter $q = m_2 \sin i / m_1$ and (o-c) is the residuals (RMS) around the Keplerian solution. The lowest $m_2 \sin i$ of $6 M_{\oplus}$ is obtained for Gl 876 d while the lowest q of 4.2×10^{-5} is achieved on μ Ara c.

References: [1] *Santos et al. (2004a)*; [2] *McArthur et al. (2004)*; [3] *Udry et al. (2006)*; [4] *Vogt et al. (2005)*; [5] *Rivera et al. (2005)*; [6] *Butler et al. (2004)*; [7] *Bonfils et al. (2005a)*.

These planetary companions, together with recently detected sub-Saturn-mass planets on intermediate-period orbits, populate the lower end of the planetary mass distribution, a region still strongly affected by detection incompleteness (Fig. 2). The discovery of very-low-mass planets so close to the detection threshold of radial-velocity surveys suggests that this kind of object may be rather common. The very existence of such planets is yet another unexpected observation for theorists. Indeed, a prediction had already been made that planets with masses between 1 and $0.1 M_{\text{Sat}}$ and semimajor axes of 0.1 to 1 AU would be rare [the so-called planet desert (*Ida and Lin, 2004a*)]. At least for the moment, observations seem to be at odds with the predictions (although very little is known about the actual populating of this hypothetical desert). In any case, the search and eventual detection of planets with even lower mass will set firmer constraints to planetary system formation and evolution models.

This detection of very-low-mass planets follows from the development of a new generation of instruments capable of radial-velocity measurements of unprecedented quality. One workhorse for high-precision work is the ESO high-resolution HARPS fiber-fed echelle spectrograph especially designed for planet-search programs and astroseismology. HARPS has already proven to be the most precise spectro-velocimeter to date, reaching an instrumental radial-velocity accuracy at the level of 1 m s^{-1} over months to years (*Mayor et al., 2003; Lovis et al., 2005*), and even better on a short-term basis (*Bouchy et al., 2005a*). The Keck telescope with an upgraded detector for the HIRES spectrometer is also approaching 1 m s^{-1} precision, with demonstrated stability since August 2004.

Another fundamental change that allowed progress in planet detection toward the very low masses is the application of a careful observing strategy to reduce the perturbing effect of stellar oscillations that can obscure the tiny reflex velocity signal induced by Neptune-mass planets.

As recently as only a couple of years ago, the behavior of the stars below 3 m s^{-1} was completely unknown. However, astroseismology observations carried out with HARPS have made it clear that the achieved precision is no longer set by instrumental characteristics but rather by the stars themselves (*Mayor et al., 2003; Bouchy et al., 2005a*). Indeed, stellar p-mode oscillations on short timescales (minutes) and stellar jitter (activity-induced noise) on longer timescales (days) can and do induce significant radial-velocity changes at the level of accuracy of the HARPS measurements. Even chromospherically quiet G and K dwarfs show oscillation modes of several tens of centimeters per second each, which might add up to radial-velocity amplitudes as large as several meters per second. As a consequence, any exposure with a shorter integration time than the oscillation period of the star, or even shorter than mode-interference variation timescales, might fall arbitrarily on a peak or on a valley of these mode interferences and thus introduce additional radial-velocity “noise.” This phenomenon could, therefore, seriously compromise the ability

to detect very-low-mass planets around solar-type stars by means of the radial-velocity technique.

To minimize these effects as much as possible, stars for very-high-precision radial-velocity measurements have first to be chosen as slowly rotating, nonevolved, and low-activity stars. Then, in order to average out stellar oscillations, the observations have to be designed to last at least 15 to 30 min on target. This strategy is now applied to stars in the “high-precision” part of the HARPS and Keck planet-search programs. An illustration of the obtained results is given by the histogram of the radial-velocity dispersion of the HARPS high-precision survey (Fig. 7). The distribution mode is just below 2 m s^{-1} , and the peak decreases rapidly toward higher values. More than 80% of the stars show dispersion smaller than 5 m s^{-1} , and more than 35% have dispersions below 2 m s^{-1} . It must be noted that the computed dispersion includes photon-noise error, wavelength-calibration error, stellar oscillations and jitter, and, in particular, “pollution” by known extrasolar planets (hatched portion of Fig. 7) and still undetected planetary companions. The recently announced $14 M_{\oplus}$ planets orbiting μ Ara (Fig. 8) and HD 4308 (Table 1) are part of this HARPS “high-precision” subsample.

3.2. Gaseous Versus Solid-Planet Properties at Short Periods

Although the number of known Neptune-mass planets is small, it is interesting to see how their orbital parameters compare with properties of giant extrasolar planets. Because of the tiny radial-velocity amplitude they induce on the

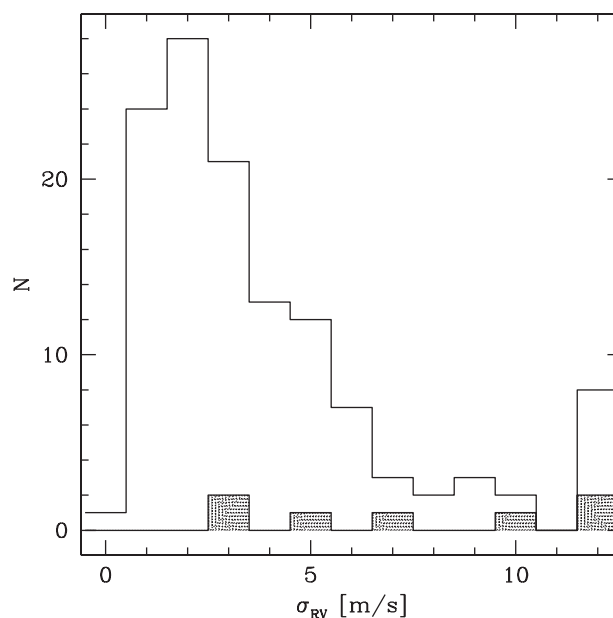


Fig. 7. Histogram of the observed radial-velocity dispersion (σ_{RV}) of the stars in the HARPS “high-precision” subprogram (124 stars with more than 3 measurements). The position of the planets detected with HARPS is indicated by the hatched area.

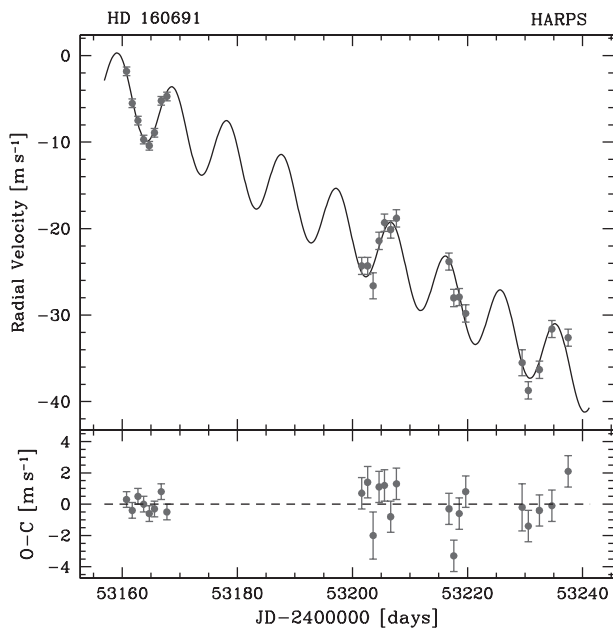


Fig. 8. HARPS measurements of μ Ara that unveiled the $14 M_{\odot}$ planet on a 9.55-d orbit. The overall r.m.s. of the residuals around the planet Keplerian solution, corrected from a long-term drift due to additional planets in the system, amounts to only 0.9 m s^{-1} , and is even as low as 0.43 m s^{-1} for the first eight points obtained by nightly averaging radial velocities measured during a one-week astroseismology campaign (Santos *et al.*, 2004a).

primary stars, limiting possible detections to short periods, a “meaningful” comparison can only be done for giant planets with periods smaller than ~ 20 d.

The distribution of short-period giant planets strongly peaks at periods around 3 d (Fig. 3). On the contrary, despite the mentioned detectability bias, the period distribution of Neptune-mass planets is rather flat up to 15 d. We also observe that orbits of Neptune-mass planets have small eccentricities (Fig. 6). In particular, for periods between 9 and 15 d (three out of the seven candidates), the mean eccentricity value is much smaller than the one of giant planets. At periods smaller than 6 d, orbits are supposed to be tidally circularized, especially if these planets are “solid.” However, among them, the largest observed eccentricities are for 55 Cnc e ($P = 2.8$ d and $e = 0.17$) and Gl 436 ($P = 2.6$ d and $e = 0.12$). The former is a member of a multiplanet system, which might explain the nonzero eccentricity of the inner small-mass planet (section 2.6); however, the problem is more difficult for the latter case. Another difference between giant and Neptune-mass planets can also be found in the parent-star metallicity distribution (see section 5.2).

Although the number of objects does not constitute a statistically significant sample, these small differences may hint that giant gaseous and “solid” planets form two distinct populations, with different properties. More detections are, however, needed to consider this question in a more convincing way.

4. MULTIPLE PLANET SYSTEMS

There are more than 170 planet-hosting stars for the more than 200 known extrasolar planets. Seventeen of these stars have multiple-planet systems rather than single planets. One further system, HD 217107, shows an additional curved drift of the residuals of the single-planet Keplerian solution that is compatible with a second planetary companion. The orbital characteristics of these systems are summarized in Table 2. The most prolific of them is 55 Cnc, with four detected planets. v And, HD 37124, Gl 876, and μ Ara (HD 160691) each have three planets. Finally, there are a total of 11 known double-planet systems.

Among planet-bearing stars, $\sim 12\%$ are known multiple-planet systems. Thus, the probability of finding a second planet is enhanced by a factor of 2 over the $\sim 6\%$ probability of finding the first planet. The fraction of known multiplanet systems is certainly a lower limit. One challenge is that low-amplitude trends from more distant, longer-period sibling planets are easily absorbed into single-planet Keplerian models. Detection of additional planets is easier in systems where the more distant planet is greater than a few times the mass of Jupiter since such systems will produce larger-velocity amplitudes. However, the mass histogram (Fig. 2) shows that high-mass planets are uncommon. A second challenge exists for systems with small orbital period ratios like Gl 876. There, dynamical interactions between planets can complicate Keplerian fitting of the observations and delay characterization and announcement of a second planet. As a result, while one orbital period is sufficient for a single-planet system with velocity amplitudes greater than 10 m s^{-1} ($\sim 3\sigma$ detection), longer phase coverage is generally required to disentangle additional components. The longest-running, high-precision survey is the 15-year planet search at Lick Observatory. This sample of 100 stars includes the multiplanet systems 55 Cnc, Ups And, Gl 876, and 47 UMa. Half the planet-hosting stars from that sample now have more than one detected planet. For the somewhat younger ELODIE planet-search program in Haute-Provence, begun in 1994 and expanded in 1996, 25% of the stars with detected planets host more than one planet.

In light of the challenges that preclude detection of multiplanet systems and given the high fraction of multiplanet systems in the older long-running search programs, it seems likely that most stars form *systems of planets* rather than isolated, single planets. New techniques, complementary to radial velocities, to discover exoplanets with imaging, interferometry, or astrometry will very probably exploit the sizable fraction of multiple-planet systems when designing their programs.

4.1. Mean-Motion-Resonance Systems

It is tempting to categorize multiplanet systems as either hierarchical or resonance systems. Among the known multiplanet systems, at least eight (nearly half) are in mean-motion resonances (MMR) and four of these are in the low-order 2:1 resonance. Figure 9 shows the ratio of orbital

TABLE 2. Orbital parameters of multiplanet systems.

Star ID	P (d)	e	$m_2 \sin i$ (M_{Jup})	a (AU)	Rem
HD 75732 b	14.67	0.02	0.78	0.115	55 Cnc
HD 75732 c	43.9	0.44	0.22	0.24	3:1 (c:b)
HD 75732 d	4517	0.33	3.92	5.26	
HD 75732 e	2.81	0.17	0.045	0.038	
HD 9826 b	4.617	0.012	0.69	0.06	v And
HD 9826 c	241.5	0.28	1.89	0.83	
HD 9826 d	1284	0.27	3.75	2.53	~16:3 (d:c)
HD 37124 b	154.5	0.06	0.61	0.53	
HD 37124 c	843.6	0.14	0.60	1.64	
HD 37124 d	2295.0*	0.2	0.66	3.19	~8:3 (d:c)
Gl 876 b	60.94	0.025	1.93	0.21	2:1 \pm 0.02 (b:c)
Gl 876 c	30.10	0.27	0.56	0.13	
Gl 876 d	1.938	0.0	0.023	0.021	
HD 160691 b	629.6	0.26	1.67	1.5	μ Ara
HD 160691 c	9.55	0.0	0.044	0.09	
HD 160691 d	2530	0.43	1.22	4.17	4:1 \pm 0.25 (d:b)
HD 12661 b	262.5	0.35	2.37	0.83	
HD 12661 c	1684	0.02	1.86	2.60	~13:2 \pm 0.8 (c:b)
HD 217107 b	7.12	0.13	1.35	0.10	
HD 217107 c	>10,000 [†]	—	>10	>20	
HD 168443 b	58.11	0.53	7.64	0.29	
HD 168443 c	1764	0.22	17.0	2.85	
HD 169830 b	225.6	0.31	2.88	0.81	
HD 169830 c	2102	0.33	4.04	3.60	
HD 190360 b	2891	0.36	1.56	3.92	
HD 190360 c	17.1	0.01	0.057	0.13	
HD 202206 b	256.2	0.43	17.5	0.83	
HD 202206 c	1297	0.28	2.41	2.44	~5:1 \pm 0.07 (c:b)
HD 38529 b	14.3	0.25	0.84	0.13	
HD 38529 c	2182	0.35	13.2	3.68	
HD 73526 b	187.5	0.39	2.07	0.66	
HD 73526 c	376.9	0.40	2.30	1.05	2:1 \pm 0.01 (c:b)
HD 74156 b	51.6	0.64	1.86	0.29	
HD 74156 c	2025	0.58	6.19	3.40	
HD 82943 b	219.5	0.39	1.82	0.75	
HD 82943 c	439.2	0.02	1.75	1.20	2:1 \pm 0.01 (c:b)
HD 95128 b	1089	0.06	2.54	2.09	47 UMa
HD 95128 c	2594	0.00	0.76	3.73	
HD 108874 b	395.4	0.07	1.36	1.05	
HD 108874 c	1606	0.25	1.02	2.68	4:1 \pm 0.1 (c:b)
HD 128311 b	458.6	0.25	2.18	1.10	
HD 128311 c	928	0.17	3.20	1.77	2:1 \pm 0.03 (c:b)

*See Vogt et al. (2005) for alternate orbital solution.

[†]Period not covered.

Values are from the literature or updated from Butler et al. (2006). Period resonances are indicated in the “Rem” column.

periods (defined as the longer period divided by the shorter period) for multiplanet systems listed in Table 2. Uncertainties in the derived orbital periods (Butler et al., 2006) are shown as error bars. Except for HD 37124, which has an uncertain Keplerian model, orbital ratios less than or equal to 4:1 are all very close to integral period ratios with low orders (MMR) of 2:1, 3:1, or 4:1. The outer two planets orbiting v And are close to a 16:3 MMR and HD 12661

may be in a 13:2 MMR. No mean-motion resonances are observed close to the exact ratio of 5:1 or 6:1. However, uncertainties in the orbital solution for HD 12661 allow for the possibility of a 6:1 MMR and the stability study of HD 202206 (Correia et al., 2005) suggests that the system is trapped in the 5:1 resonance. In this latter case the 5:1 resonance could indicate that the planet formed in a circum-binary disk, as the inner “planet” has a minimum mass of

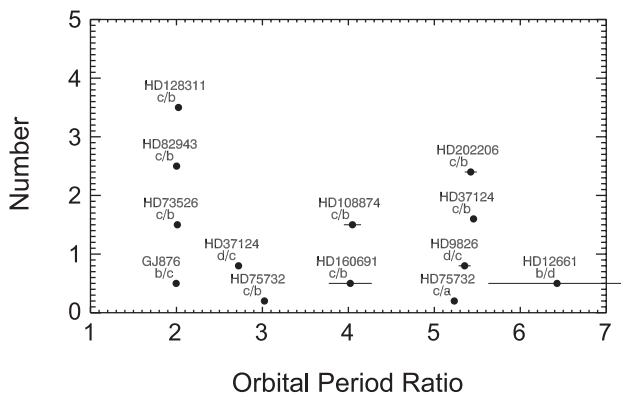


Fig. 9. The ratio of longer to shorter orbital periods is shown for multiplanet systems in Table 2. Uncertainties in the orbital periods are propagated as error bars in the period ratio. The low-order MMR at 2:1 appears to be quite narrow with $2 \pm 0.01:1$. Four of the 18 systems (including uncovered periods) reside in a 2:1 resonance.

$17 M_{\text{Jup}}$. Beyond the 4:1 MMR, the orbital period ratios quickly stray from integral ratios. This suggests that if planets are close enough, it is likely that resonance capture will occur. Conversely, resonance capture seems less effective if the orbital period ratio is greater (i.e., the planets do not make a close approach), although longer orbital periods are not as precisely determined.

Kley et al. (2004) model the resonant capture of planets and find that for the 2:1 MMR, their models predict (1) a larger mass for the outer planet, and (2) higher eccentricity for the inner planet. We find that the orbital eccentricity is higher for the inner planet in three of the four 2:1 resonance systems. In the fourth system, HD 73526, the eccentricities for both components are comparable. We find that the outer planet is more massive (assuming coplanar orbits) in GJ 876 and HD 128311. The outer planet is only slightly more massive in HD 73526, and it is slightly less massive in the Keplerian model for HD 82943 (*Mayor et al.*, 2004).

The orbital parameters of multiplanet systems seem indistinguishable from those of single-planet systems. For example, Figs. 4 and 6 compare the period mass and eccentricity distributions of multiple- and single-planet systems.

4.2. Dynamics: Planet-Planet Interactions

The presence of two or more interacting planets in a system dramatically increases our potential ability to constrain and understand the processes of planetary formation and evolution. Short-term dynamical interactions are of particular interest because of the directly observable consequences. Among them, the observed $P_i/P_j = 2/1$ resonant systems are very important because, when the planet orbital separations are not too large, planet-planet gravitational interactions become nonnegligible during planetary “close” encounters, and will noticeably influence the system evolution on a timescale on the order of a few times the long period. The radial-velocity variations of the central star will

then differ substantially from velocity variations derived assuming the planets are executing independent Keplerian motions (Fig. 10). In the most favorable cases, the orbital-plane inclinations, not otherwise known from the radial-velocity technique, can be constrained since the amplitude of the planet-planet interaction directly scales with their true masses. Several studies have been conducted in this direction for the GJ 876 system (*Laughlin et al.*, 2005; *Rivera et al.*, 2005) hosting two planets at fairly small separations (2/1 resonance). The results of the Newtonian modeling of the GJ 876 system have validated the method, improving notably the determination of the planetary orbital elements and also unveiling the small-mass planet embedded in the very inner region of the system (Tables 1 and 2).

Another useful application of the dynamical analysis of a multiplanet system is the localization of the resonances in the system that shape its overall structure. Stability studies are also mandatory to ensure the long-term viability of the systems observed now.

5. PRIMARY STAR PROPERTIES

Additional information to constrain planet-formation models comes from the study of the planet hosts themselves. In particular, the mass and metallicity of the parent stars seem to be of prime importance for models of planet formation (*Ida and Lin*, 2004b, 2005; *Benz et al.*, 2005).

5.1. Metallicity Correlation of Stars with Giant Planets

A correlation between the presence of Doppler-detected gas giant planets and high metallicity in the host stars was noted in the early years of extrasolar planet detection (*Gonzalez*, 1997, 1998; *Gonzalez et al.*, 1999; *Gonzalez and Laws*, 2000; *Fuhrmann et al.*, 1997, 1998; *Santos et al.*,

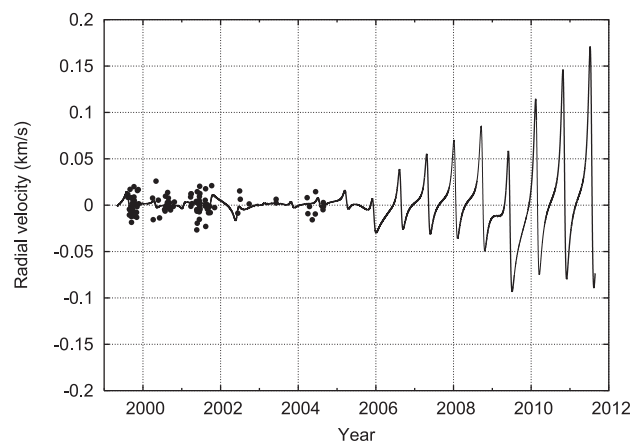


Fig. 10. Temporal differences between the radial velocities predicted by the two-Keplerian models and the numerical integration of the system HD 202206 (*Correia et al.*, 2005). Residuals of the CORALIE measurements around the Keplerian solution are displayed as well.

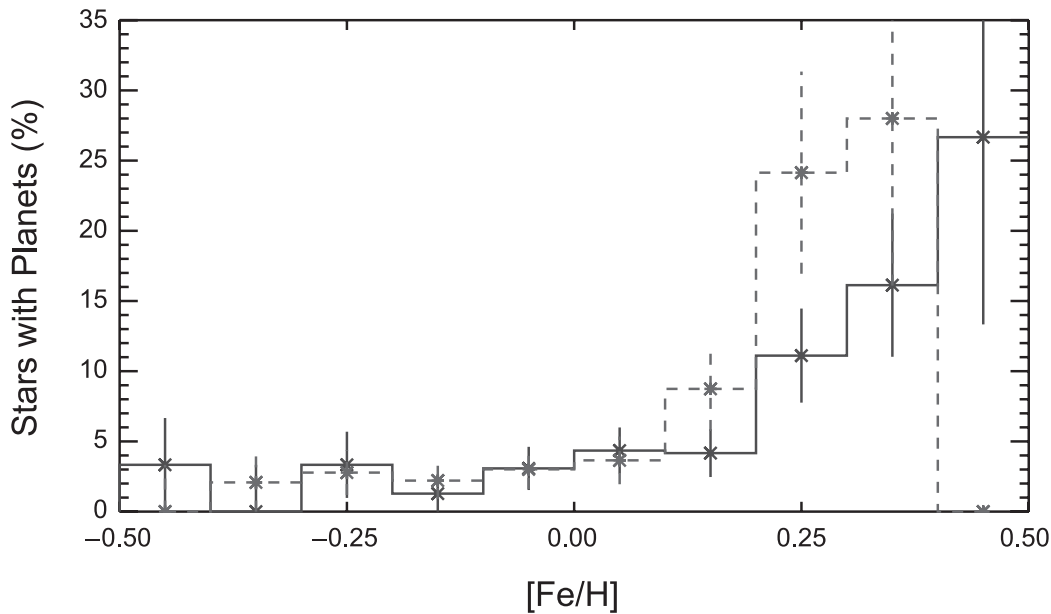


Fig. 11. The percentage of stars with exoplanets is shown as a function of stellar metallicity. Here, the dashed line shows the results of Santos et al. (2004b) for 875 CORALIE nonbinary stars and the solid line shows the analysis of 1040 Lick, Keck, and AAT stars (Fischer and Valenti, 2005). Although based on different metallicity estimates and on different star samples, the two distributions agree within the error bars.

2000, 2003). This observation led to debate over the origin of the planet-metallicity correlation. One explanation posited that high metallicity enhanced planet formation because of the increased availability of small particle condensates, the building blocks of planetesimals. Another argument suggested that enhanced stellar metallicity could be pollution of the stellar convective zone resulting from late-stage accretion of gas-depleted material. A third explanation invoking the possibility that planet migration is somewhat controlled by the dust content of the disk — thus leading to an observed bias in favor of close-in planets around metal-rich stars — seems to be reasonably ruled out by current models (Livio and Pringle, 2003). The two main mechanisms result in different stellar structures; in the first case, the star is metal-rich throughout, while in the latter case, the convective zone has significantly higher metallicity than the stellar interior.

At the time of the early observation of the planet metallicity correlation only a handful of planet-bearing stars were known, and the comparison metallicity distributions came from volume-limited studies, carried out by different researchers at a time when systematic offsets of 0.1 dex in metallicity results were common. Eventually, systematic, homogeneous studies of all stars on planet-search surveys were completed (Santos et al., 2001) with the further requirement that the stars have enough observations to have found a Jupiter-like planet with an orbital period out to 4 yr (Fischer et al., 2004; Santos et al., 2004b, 2005; Fischer and Valenti, 2005). Rather than checking the metallicity of planet-bearing stars, the presence of gas giant planets orbiting stars with known metallicity was assessed for well

over 1500 stars on ongoing Doppler planet surveys. Figure 11 shows the percentage of stars with planets as a function of metallicity from 1040 stars on the Lick, Keck, and AAT planet surveys [solid line (Fischer and Valenti, 2005)] and the percentage of stars with planets from 875 stars on the CORALIE survey [nonbinary and with more than five observations; dashed line (Santos et al., 2004b)]. The occurrence of planets as a function of metallicity was fit by Fischer and Valenti (2005) with a power law

$$\mathcal{P}(\text{planet}) = 0.03 \times \left(\frac{(N_{\text{Fe}}/N_{\text{H}})}{(N_{\text{Fe}}/N_{\text{H}})_{\odot}} \right)^2$$

Thus, the probability of forming a gas giant planet is roughly proportional to the square of the number of metal atoms, and increases by a factor of 5 when iron abundance is increased by a factor of 2, from $[\text{Fe}/\text{H}] = 0$ to $[\text{Fe}/\text{H}] = 0.3$.

The self-consistent analysis of high-resolution spectra for more than 1500 stars on planet-search surveys also distinguished between the two enrichment hypotheses. Metallicity was not observed to increase with decreasing convective zone depth for main-sequence stars, suggesting that pollution through accretion was not responsible for the observed metallicity enhancement of planet-bearing stars. This argument is, however, questioned by Vaclair (2004), invoking thermohaline convection (metallic fingers) that might dilute the accreted matter inside the star and thus reconcile the overabundances expected in the case of accretion of planetary material with the observations of stars of different masses. Even more important in terms of discarding the pollution hypothesis, the analysis of subgiants in the sample

showed that subgiants with planets had high metallicity, while subgiants without detected planets had a metallicity distribution similar to main-sequence stars without detected planets. Since significant mixing of the convective zone takes place along the subgiant branch, subgiants would have diluted accreted metals in the convective zone. The fact that high metallicity persisted in subgiants with planets demonstrated that these stars were metal-rich throughout. The existence of a planet metallicity correlation supports core accretion over gravitational instability as the formation mechanism for gas giant planets with orbital periods as long as 4 yr.

The observed relation between stellar metal content and planet occurrence has motivated metallicity-biased planet-search programs targeting short-period planets to look for hot Jupiters, which are ideal candidates for a photometric transit-search followup. These surveys are successful (*Fischer et al.*, 2005; *Sato et al.*, 2005; *Bouchy et al.*, 2005b; *Da Silva et al.*, 2006) (see section 6). However, the built-in bias of the sample has to be kept in mind when examining possible statistical relations between the star metallicity and other orbital or stellar parameters. Up to now, no clear correlation between metallicity and orbital parameters has been observed.

5.2. Metallicity of Stars Hosting Neptune-Mass Planets

It is well established that the detected giant planets preferentially orbit metal-rich stars. What is the situation for the newly found Neptune-mass planets? If, as proposed by several authors (see, e.g., *Lecavelier et al.*, 2004; *Baraffe et al.*, 2004, 2005, and references therein), the new *hot-Neptune* planets are the remains of evaporated ancient giant planets, their host stars should also follow the metallicity trend observed for their giant progenitor hosts. This does not seem to be the case, considering that the seven known planets with $m_2 \sin i \leq 21 M_{\oplus}$ (Table 1) have metallicities of 0.33, 0.35, 0.02, 0.14, -0.03 , -0.25 , and -0.31 , respectively [the metallicity of the three M dwarfs comes from the photometric calibration derived by *Bonfils et al.* (2005b)]. Although the statistics are still poor, the spread of these values over the nearly full range of planet-host metallicities (Fig. 12) suggests a different relation between metal content and planet frequency for the icy/rocky planets in regard to the giant ones.

It is worth remarking that three of the Neptune-mass candidates orbit M-dwarf primaries. Recent Monte Carlo simulations by *Ida and Lin* (2005) show that planet formation around small-mass primaries tends to form planets with lower masses in the Uranus/Neptune domain. A similar result that favors lower-mass planets is also observed for solar-type stars in the case of the low metallicity of the protostellar nebula (*Ida and Lin*, 2004b; *Benz et al.*, 2005). Future developments in the planet-formation models and new detections of very-low-mass planets will help to better understand these two converging effects.

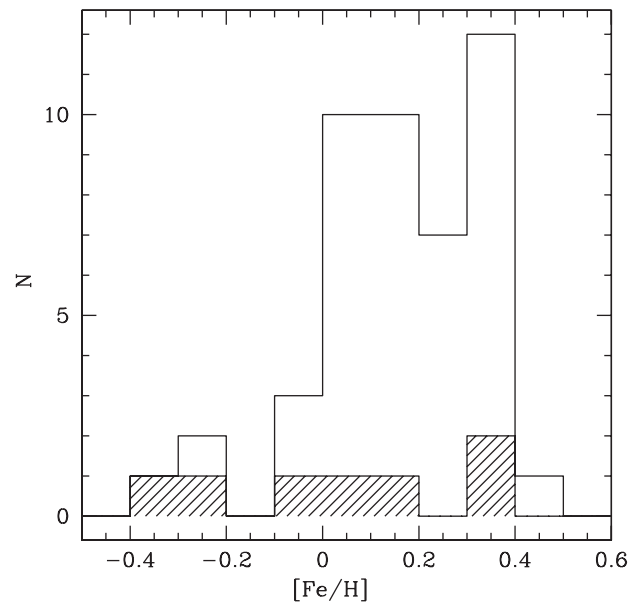


Fig. 12. Metallicity distribution of the sample of extrasolar planet hosts for planets with shorter periods than 20 d. Stars with Neptune-mass planets are indicated by the shaded portion of the histogram.

5.3. Primary Mass Effect

The mass of the primary star also appears to be an important parameter for planet-formation processes. In the case of low-mass stars, results from ongoing surveys indicate that giant gaseous planets are rare around M dwarfs in comparison to FGK primaries. The only known system with two giant planets is Gl 876 (Table 2). In particular, no hot Jupiter has been detected close to an M dwarf. This result, however, still suffers from small number statistics. On the other hand, as seen above, three of the five planets found to orbit an M dwarf have masses below $21 M_{\oplus}$ and are probably “solid” planets. Thus, the occurrence rate for planets around M dwarfs appears to be directly dependent on the domain of planet masses considered.

For more massive primaries, new surveys targeting earlier, rotating A–F dwarfs (*Galland et al.*, 2005a,b) and programs surveying G–K giant stars (*Setiawan et al.*, 2005; *Sato et al.*, 2004; *Hatzes et al.*, 2005) are starting to provide interesting candidates. The detected planets are generally massive ($>5 M_{\text{Jup}}$), but it is still too early to reach a conclusion about a “primary mass” effect as those programs are still strongly observationally biased (larger-mass primaries and short time baseline for the surveys).

6. FOLLOWUP OF TRANSITING PLANETS

In recent years, groundbased transit searches have produced a number of planetary transiting candidates (see the chapter by Charbonneau et al.). The most successful of these searches to date has been the OGLE survey, which

announced close to 180 possible transiting planets (Udalski et al., 2002a,b). These new detections stimulated intensive followup observations to detect the radial-velocity signatures induced by the orbiting body. Surprisingly, these studies revealed that most of the systems were rather eclipsing binaries of small stars (M dwarfs) in front of F–G dwarfs, eclipsing binaries in blended multiple stellar systems (triple, quadruple), or grazing stellar eclipses, all mimicking photometric planetary transits (Bouchy et al., 2005c; Pont et al., 2005). The spectroscopic followup demonstrated the difficulty of the interpretation of shallow transit lightcurves without complementary radial-velocity measurements. The magnitude of the OGLE planetary candidates ranges from $V \sim 16$ to 17.5; close to the faint capability of an accurate fibered spectrograph like FLAMES on the VLT and probably beyond the capability of slit spectroscopy with iodine self-calibration. This implies that a deeper photometric transit survey would face serious difficulties in confirming the planetary nature of the transiting object by Doppler followup.

To date, six planets have been detected from transit surveys and confirmed by radial velocities. Five of these have been found by the OGLE survey (Udalski et al., 2002a,b) and one by the TrES network (Alonso et al., 2004). Three of the OGLE planets have periods smaller than 2 d (very hot Jupiters). Such short periods, although easy to detect, are not found in the radial-velocity surveys, suggesting that those objects are about 10× less numerous than hot Jupiters [$2.5 \leq P \leq 10$ d (Gaudi et al., 2005)]. In addition to the photometrically detected planets, three planets identified by radial-velocity measurements have been found transiting in front of their parent stars.

When transit photometry is combined with high-precision radial-velocity measurements, it is possible to derive an accurate mass and radius (Table 3) as well as the mean planet density. These important values constrain planetary interior models as well as the planet-evolution history. It is interesting to note here that the majority of planets for which we know both mass and radius have been found by transit survey despite the fact that more than 200 planets have been identified by radial-velocity searches. This is a consequence

TABLE 3. List of planets with both radius (from transit) and mass estimate (from accurate radial velocities).

Object	Period (d)	Mass (M_{Jup})	Radius (R_{Jup})
OGLE-TR-10 b	3.101	0.63 ± 0.14	1.31 ± 0.09
OGLE-TR-56 b	1.212	1.24 ± 0.13	1.25 ± 0.08
OGLE-TR-111 b	4.016	0.52 ± 0.13	0.97 ± 0.06
OGLE-TR-113 b	1.432	1.35 ± 0.22	1.08 ± 0.06
OGLE-TR-132 b	1.690	1.19 ± 0.13	1.13 ± 0.08
TrES-1	3.030	0.73 ± 0.04	1.08 ± 0.05
HD 209458 b	3.525	0.66 ± 0.01	1.355 ± 0.005
HD 189733 b	2.219	1.15 ± 0.04	1.26 ± 0.08
HD 149026 b	2.876	0.33 ± 0.02	0.73 ± 0.06

Data from Alonso et al. (2004); Moutou et al. (2004); Pont et al. (2004, 2005); Bouchy et al. (2005b,c); Winn et al. (2005).

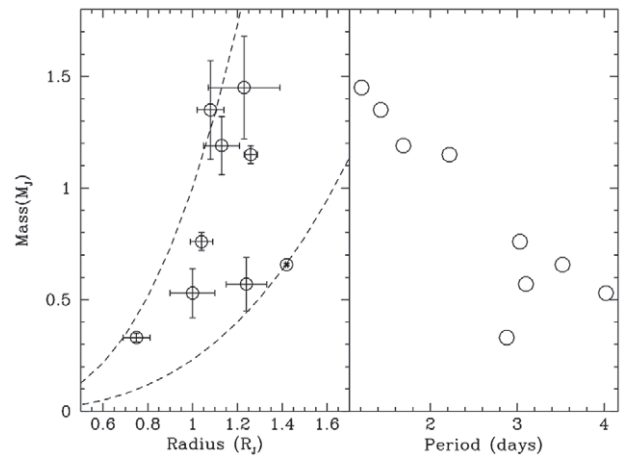


Fig. 13. Mass-radius and mass-period diagrams of transiting planets with radius and accurate mass estimates. On the left panel, the dashed lines indicate isodensity contours of 0.3 and 1.3 g cm^{-3} .

of the low probability of finding a transiting configuration among the planets found by radial-velocity surveys, while most of all the transiting candidates found so far can be followed up with radial-velocity measurements. On the other hand, the three planets transiting the brightest stars have been found first by radial velocities as transit surveys are mainly targeting crowded fields with fainter stars.

The derived density of transiting extrasolar planets covers a surprisingly wide range of values from 0.3 to 1.3 g cm^{-3} (Fig. 13). The “problem” of the anomalously large radius and low density of HD 209458 b is clearly not shared by all very close planets since planets with a similar mass are found to have a different density. This demonstrates a surprising diversity and reveals our lack of detailed understanding of the physics of irradiated giant planets.

The distribution of planets in a period vs. mass diagram shows an intriguing correlation (Fig. 13). Transiting planets seem to lie on a well-defined line of mass decreasing with increasing orbital period. This puzzling observation, pointed out by Mazeh et al. (2005), could be the consequence of mechanisms such as thermal evaporation (Lecavelier et al., 2004; Baraffe et al., 2004, 2005) or Roche limit mass transfer (Ford and Rasio, 2005). It is worth noting the location of HD 149026 b, below the relation, that could be a result of its different structure with a large core (Sato et al., 2005; Charbonneau et al., 2006). Even more surprising in the diagram is the complete lack of candidates above the relation. Why are we missing more massive transiting planets at $P = 3\text{--}4$ d? No convincing explanation has been proposed yet for this puzzling observation.

7. THE FUTURE OF RADIAL VELOCITIES

An important lesson from the past few years is that the radial-velocity technique has not reached its “limits” yet in the domain of exoplanets. In fact, the future of radial velocity studies is still bright.

1. Recent discoveries indicate that a population of Neptune- and Saturn-mass planets remains to be discovered below 1 AU. The improved precision of the radial velocity surveys will address this issue in the near future, thereby providing us with useful new constraints on planet-formation theories. With the precision level now achieved for radial-velocity measurements, a new field in the search for extrasolar planets is at hand, allowing the detection of companions of a few Earth masses around solar-type stars. Very-low-mass planets ($<10 M_{\oplus}$) might be more frequent than the previously found giant worlds.

2. As described above, radial-velocity followup measurements are mandatory to determine the mass of transiting companions and then to calculate their mean densities. These observations establish the planetary nature of the companions and provide important parameters to constrain planetary atmosphere and interior models. This is important in view of the expected results of the space missions COROT and Kepler, which should provide hundreds of transiting planets of various sizes and masses. When a transit signal is detected, the orbital period is then known. As a result, radial-velocity followup is less demanding, both in terms of the number and precision of the acquired Doppler measurements. For example, a $2 M_{\oplus}$ planet on a 4-d orbit induces on a Sun-mass star a radial-velocity amplitude of about 80 cm s^{-1} that will be possible to detect with only a “few” high-precision radial-velocity measurements, provided that the period of the system is known in advance. In this context, the most exciting aspect is the opportunity to explore the mass-radius relation down to the Earth-mass domain.

3. The threshold of the lowest-mass planet detectable by the Doppler technique keeps decreasing. The domain below the 1 m s^{-1} level has not yet been explored. Results obtained with the HARPS spectrograph show that, even if stars are intrinsically variable in radial velocity (at modest levels) due to acoustic modes, it is nevertheless possible on the short term to reach precisions well below 1 m s^{-1} by applying an adequate observational strategy. One open issue, however, remains unsolved: the behavior of the stars on a longer timescale, where stellar jitter and spots may impact the final achievable accuracy. In this case, an accurate pre-selection of the stars is needed to select good candidates and optimize the use of telescope time. In addition, line bisector analysis and followup of activity indicators such as $\log(R'_{\text{HK}})$, as well as photometric measurements, may flag suspect results.

The discovery of an extrasolar planet by means of the Doppler technique requires either that the radial-velocity signal induced by the planet is significantly higher than the dispersion, or that very-high-cadence observations are obtained. A large number of observations with excellent phase coverage is critical for ruling out false positives, particularly given the relatively high number of free parameters in the orbital solution for multiplanet systems. A large number of measurements will help to mitigate the challenges of low-amplitude detections, but will demand an enormous investment of observing time. Thus, as long as we are willing to devote sufficient resources in terms of telescope time

and advance designed spectrographs (high-level temperature and pressure control), it should in principle be possible to detect Earth-like planets (Pepe et al., 2005).

Note added in proof: During the production of this volume, a system with three Neptune-mass planets has been discovered around HD 69830 (Lovis et al., 2006), as well as four transiting planets (McCullough et al., 2006; Bakos et al., 2006; Cameron et al., 2006), significantly enlarging two small-statistic subsamples of meaningful exoplanets.

REFERENCES

- Alibert Y., Mordasini C., and Benz W. (2004) *Astron. Astrophys.*, 417, L25–L28.
- Alibert Y., Mordasini C., Benz W., and Winisdoerffer C. (2005) *Astron. Astrophys.*, 434, 343–353.
- Alonso R., Brown T., Torres G., Latham D., Sozzetti A., et al. (2004) *Astrophys. J.*, 613, L153–L156.
- Bakos G. A., et al. (2006) *Astrophys. J.*, in press.
- Baraffe I., Selsis F., Chabrier G., Barman T., Allard F., Hauschildt P. H., and Lammer H. (2004) *Astron. Astrophys.*, 419, L13–L16.
- Baraffe I., Chabrier G., Barman T., Selsis F., Allard F., and Hauschildt P. H. (2005) *Astron. Astrophys.*, 436, L47–L51.
- Benz W., Mordasini C., Alibert Y., and Naef D. (2005) In *Tenth Anniversary of 51 Peg b: Status of and Prospects for Hot Jupiter Studies* (L. Arnold et al., eds.), pp. 24–34. Frontier Group, Paris.
- Bodenheimer P., Hubickyj O., and Lissauer J. (2000) *Icarus*, 143, 2–14.
- Bonfils X., Forveille T., Delfosse X., Udry S., Mayor M., et al. (2005a) *Astron. Astrophys.*, 443, L15–L18.
- Bonfils X., Delfosse X., Udry S., Santos N. C., Forveille T., and Ségransan D. (2005b) *Astron. Astrophys.*, 442, 635–642.
- Bouchy F., Bazot M., Santos N. C., Vauclair S., and Sosnowska D. (2005a) *Astron. Astrophys.*, 440, 609–614.
- Bouchy F., Udry S., Mayor M., Moutou C., Pont F., Iribarne N., et al. (2005b) *Astron. Astrophys.*, 444, L15–L19.
- Bouchy F., Pont F., Melo C., Santos N. C., Mayor M., Queloz D., and Udry S. (2005c) *Astron. Astrophys.*, 431, 1105–1121.
- Butler P., Marcy G., Vogt S., and Fischer D. (2000) In *Planetary Systems in the Universe* (A. Penny et al., eds), p. 1. IAU Symposium 202, ASP, San Francisco.
- Butler P., Vogt S., Marcy G., Fischer D., Wright J., et al. (2004) *Astrophys. J.*, 617, 580–588.
- Butler P., Wright J., Marcy G., Fischer D., Vogt S., et al. (2006) *Astrophys. J.*, 646, 505–522.
- Cameron A. C., et al. (2006) *Mon. Not. R. Astron. Soc.*, in press.
- Charbonneau D., Winn J., Latham D., Bakos G., Falco E., et al. (2006) *Astrophys. J.*, 636, 445–452.
- Correia A., Udry S., Mayor M., Laskar J., Naef D., et al. (2005) *Astron. Astrophys.*, 440, 751–758.
- Cumming A., Marcy G., and Butler P. (1999) *Astrophys. J.*, 526, 890–915.
- Da Silva R., Udry S., Bouchy F., Mayor M., Moutou C., et al. (2006) *Astron. Astrophys.*, 446, 717–722.
- Eggenberger A., Udry S., and Mayor M. (2004) *Astron. Astrophys.*, 417, 353–360.
- Endl M., Kürster M., Els S., Hatzes A., Cochran W., et al. (2002) *Astron. Astrophys.*, 392, 671–690.
- Fischer D. and Valenti J. (2005) *Astrophys. J.*, 622, 1102–1117.
- Fischer D., Valenti J., and Marcy G. (2004) In *Stars as Suns: Activity, Evolution and Planets* (A. Dupree and A. Benz, eds.), p. 29. IAU Symposium 219, ASP, San Francisco.
- Fischer D., Laughlin G., Butler P., Marcy G., Johnson J., et al. (2005) *Astrophys. J.*, 620, 481–486.
- Ford E. and Rasio F. (2005) In *PPV Poster Proceedings*, www.lpi.usra.edu/meetings/ppv2005/pdf/8360.pdf.
- Ford E., Havlickova M., and Rasio F. (2001) *Icarus*, 150, 303–313.
- Ford E., Rasio F., and Yu K. (2003) In *Scientific Frontiers in Research on Extrasolar Planets* (D. Deming and S. Seager, eds.), pp. 181–188. ASP Conf. Series 294, San Francisco.

- Fuhrmann K., Pfeiffer M., and Bernkopf J. (1997) *Astron. Astrophys.*, 326, 1081–1089.
- Fuhrmann K., Pfeiffer M., and Bernkopf J. (1998) *Astron. Astrophys.*, 336, 942–952.
- Galland F., Lagrange A.-M., Udry S., Chelli A., Pepe F., et al. (2005a) *Astron. Astrophys.*, 443, 337–345.
- Galland F., Lagrange A.-M., Udry S., Chelli A., Pepe F., et al. (2005b) *Astron. Astrophys.*, 444, L21–L24.
- Gaudi B. S., Seager S., and Mallen-Ornelas G. (2005) *Astrophys. J.*, 623, 472–481.
- Gonzalez G. (1997) *Mon. Not. R. Astron. Soc.*, 285, 403–412.
- Gonzalez G. (1998) *Astron. Astrophys.*, 334, 221–238.
- Gonzalez G. and Laws C. (2000) *Astron. J.*, 119, 390–396.
- Gonzalez G., Wallerstein G., and Saar S. (1999) *Astrophys. J.*, 511, L111–L114.
- Halbwachs J.-L., Mayor M., Udry S., and Arenou F. (2003) *Astron. Astrophys.*, 397, 159–175.
- Halbwachs J.-L., Mayor M., and Udry S. (2005) *Astron. Astrophys.*, 431, 1129–1137.
- Hatzes A. P., Guenther E., Endl M., Cochran W., Döllinger M., and Bedalov A. (2005) *Astron. Astrophys.*, 437, 743–751.
- Ida S. and Lin D. (2004a) *Astrophys. J.*, 604, 388–413.
- Ida S. and Lin D. (2004b) *Astrophys. J.*, 616, 567–672.
- Ida S. and Lin D. (2005) *Astrophys. J.*, 626, 1045–1060.
- Jorissen A., Mayor M., and Udry S. (2001) *Astron. Astrophys.*, 379, 992–998.
- Kley W., Peitz J., and Bryden G. (2004) *Astron. Astrophys.*, 414, 735–747.
- Laughlin G., Butler P., Fischer D., Marcy G., Vogt S., and Wolf A. (2005) *Astrophys. J.*, 612, 1072–1078.
- Lecavelier des Etangs A., Vidal-Madjar A., McConnell J. C., and Hebrard G. (2004) *Astron. Astrophys.*, 418, L1–L4.
- Levison H. F., Lissauer J., and Duncan M. J. (1998) *Astron. J.*, 116, 1998–2014.
- Lin D. and Ida S. (1997) *Astrophys. J.*, 477, 781–791.
- Lin D., Bodenheimer P., and Richardson D. C. (1996) *Nature*, 380, 606–607.
- Livio M. and Pringle J. E. (2003) *Mon. Not. R. Astron. Soc.*, 346, L42–L44.
- Lovis C., Mayor M., Bouchy F., Pepe F., Queloz D., et al. (2005) *Astron. Astrophys.*, 437, 1121–1126.
- Lovis C., Mayor M., Pepe F., Alibert Y., Benz W., et al. (2006) *Nature*, 441, 305–309.
- Marcy G., Cochran W., and Mayor M. (2000) In *Protostars and Planets IV* (V. Mannings et al., eds.), pp. 1285–1311. Univ. of Arizona, Tucson.
- Marcy G., Butler P., Vogt S., Liu M., Laughlin G., et al. (2001) *Astrophys. J.*, 555, 418–425.
- Marcy G., Butler P., Fischer D., Vogt S., Wright J., et al. (2005) *Prog. Theor. Phys. Suppl.*, 158, 24–42.
- Marzari F. and Weidenschilling S. J. (2002) *Icarus*, 156, 570–579.
- Mayor M. and Queloz D. (1995) *Nature*, 378, 355–358.
- Mayor M., Pepe F., Queloz D., Bouchy F., Rupprecht G., et al. (2003) *The Messenger*, 114, 20–24.
- Mayor M., Udry S., Naef D., Pepe F., Queloz D., et al. (2004) *Astron. Astrophys.*, 415, 391–402.
- Mazeh T., Krzysowski Y., and Rosenfeld G. (1997) *Astrophys. J.*, 477, L103–L106.
- Mazeh T., Zucker S., and Pont F. (2005) *Mon. Not. R. Astron. Soc.*, 356, 955–957.
- McArthur B., Endl M., Cochran W., Benedict G. F., Fischer D., et al. (2004) *Astrophys. J.*, 614, L81–L84.
- McCullough P. R., Stys J. E., Valenti J. A., Johns-Krull C. M., Janes K. A., et al. (2006) *Astrophys. J.*, 648, 1228–1238.
- Moutou C., Pont F., Bouchy F., and Mayor M. (2004) *Astron. Astrophys.*, 424, L31–L34.
- Mugrauer M., Neuhäuser R., Mazeh T., Alves J., and Guenther E. (2004) *Astron. Astrophys.*, 425, 249–253.
- Mugrauer M., Neuhäuser R., Seifahrt A., Mazeh T., and Guenther E. (2005) *Astron. Astrophys.*, 440, 1051–1060.
- Naef D., Mayor M., Beuzit J.-L., Perrier C., Queloz D., Sivan J.-P., and Udry S. (2005) In *13th Cool Stars, Stellar Systems and the Sun* (F. Favata et al., eds.), pp. 833–836. ESA SP-560, Noordwijk, The Netherlands.
- Nelson R., Papaloizou J., Masset F., and Kley W. (2000) *Mon. Not. R. Astron. Soc.*, 318, 18–36.
- Patience J., White R. J., Ghez A., McCabe C., McLean I., et al. (2002) *Astrophys. J.*, 581, 654–665.
- Pätzold M. and Rauer H. (2002) *Astrophys. J.*, 568, L117–L120.
- Pepe F., Mayor M., Queloz D., Benz W., Bertaux J.-L., et al. (2005) *The Messenger*, 120, 22–25.
- Pollack J. B., Hubickyj O., Bodenheimer P., Lissauer J., Podolak M., and Greenzweig Y. (1996) *Icarus*, 124, 62–85.
- Pont F., Bouchy F., Queloz D., Santos N. C., Melo C., Mayor M., and Udry S. (2004) *Astron. Astrophys.*, 426, L15–L18.
- Pont F., Bouchy F., Melo C., Santos N. C., Mayor M., Queloz D., and Udry S. (2005) *Astron. Astrophys.*, 438, 1123–1140.
- Rasio F. and Ford E. (1996) *Science*, 274, 954–956.
- Rivera E. J., Lissauer J., Butler P., Marcy G., Vogt S., et al. (2005) *Astrophys. J.*, 634, 625–640.
- Safronov V. S. (1969) *Evoliutsiia Doplanetnogo Oblaka*, Izdatel'stvo Nauka, Moscow.
- Santos N. C., Israelian G., and Mayor M. (2000) *Astron. Astrophys.*, 363, 228–238.
- Santos N. C., Israelian G., and Mayor M. (2001) *Astron. Astrophys.*, 373, 1019–1031.
- Santos N. C., Israelian G., Mayor M., Rebolo R., and Udry S. (2003) *Astron. Astrophys.*, 398, 363–376.
- Santos N. C., Bouchy F., Mayor M., Pepe F., Queloz D., et al. (2004a) *Astron. Astrophys.*, 426, L19–L23.
- Santos N. C., Israelian G., and Mayor M. (2004b) *Astron. Astrophys.*, 415, 1153–1166.
- Santos N. C., Israelian G., Mayor M., Bento J., Almeida P., et al. (2005) *Astron. Astrophys.*, 437, 1127–1133.
- Sato B., Ando H., Kambe E., Takeda Y., Izumiura H., et al. (2004) *Astrophys. J.*, 597, L157–L160.
- Sato B., Fischer D., Henry G., Laughlin G., Butler P., et al. (2005) *Astrophys. J.*, 633, 465–473.
- Setiawan J., Rodmann J., da Silva L., Hatzes A., Pasquini L., et al. (2005) *Astron. Astrophys.*, 437, L31–L34.
- Takeda G. and Rasio A. (2005) *Astrophys. J.*, 627, 1001–1010.
- Tremaine S. and Zakamska N. (2004) In *The Search for Other Worlds* (S. S. Holt and D. Deming, eds.), pp. 257–260. AIP Conf. Proc. 713, New York.
- Trilling D. E., Benz W., Guillot T., Lunine J., Hubbard W., Burrows A., et al. (1998) *Astrophys. J.*, 500, 428–439.
- Trilling D. E., Lunine J., and Benz W. (2002) *Astron. Astrophys.*, 394, 241–251.
- Udalski A., Paczynski B., Zebrun K., Szymanski M., Kubiak M., et al. (2002a) *Acta Astron.*, 52, 1–37.
- Udalski A., Zebrun K., Szymanski M., Kubiak M., Soszynski I., et al. (2002b) *Acta Astron.*, 52, 115–128.
- Udry S., Mayor M., Naef D., Pepe F., Queloz D., et al. (2000) *Astron. Astrophys.*, 356, 590–598.
- Udry S., Mayor M., Naef D., Pepe F., Queloz D., Santos N. C., and Burnet M. (2002) *Astron. Astrophys.*, 390, 267–279.
- Udry S., Mayor M., and Santos N. C. (2003) *Astron. Astrophys.*, 407, 369–376.
- Udry S., Mayor M., Benz W., Bertaux J.-L., Bouchy F., et al. (2006) *Astron. Astrophys.*, 447, 361–367.
- Vauclair S. (2004) *Astrophys. J.*, 605, 874–879.
- Vogt S., Butler P., Marcy G., Fischer D., Henry G., et al. (2005) *Astrophys. J.*, 632, 638–658.
- Ward W. (1997) *Icarus*, 126, 261–281.
- Weidenschilling S. J. and Marzari F. (1996) *Nature*, 384, 619–621.
- Winn J., Noyes R. W., Holman M., Charbonneau D., Ohta Y., et al. (2005) *Astrophys. J.*, 631, 1215–1226.
- Wuchterl G., Guillot T., and Lissauer J. (2000) In *Protostars and Planets IV* (V. Mannings et al., eds.), pp. 1081–1109. Univ. of Arizona, Tucson.
- Zakamska N. and Tremaine S. (2004) *Astron. J.*, 128, 869–877.
- Zucker S. and Mazeh T. (2002) *Astrophys. J.*, 568, L113–L116.